Structural Transitions in the Scaffolding and Coat Proteins of P22 Virus during Assembly and Disassembly†

Roman Tuma,‡ Peter E. Prevelige, Jr.,§ and George J. Thomas, Jr.*,‡

Division of Cell Biology and Biophysics, School of Biological Sciences, University of Missouri−Kansas City, Kansas City, Missouri 64110-2499, and Department of Microbiology, University of Alabama at Birmingham, Birmingham, Alabama 35294

Received November 27, 1995; Revised Manuscript Received February 14, 1996⊗

ABSTRACT: An *in vitro* system for investigating the assembly of the *Salmonella* phage P22 has been exploited to elucidate the structural basis of recognition between scaffolding protein (gp8) and coat protein (gp5) subunits of the viral procapsid. Raman spectroscopy and circular dichroism have been employed to examine structural thermostabilities of both gp8 and gp5 in native procapsids, and to characterize structural changes accompanying scaffolding exit, procapsid expansion, and shell disassembly. It is found that the secondary structure of the isolated gp8 subunit is rich in α-helix (≈40%), is highly thermolabile, and is characterized by *noncooperative* unfolding ($T_m \approx 49$ °C). Conversely, the procapsid-bound gp8 subunit exhibits stabilization of its α-helical secondary structure, characterized by *cooperative* unfolding. Because cooperative unfolding of gp8 coincides with exit from the procapsid, the present results suggest that unfolding and release are coupled processes. Structural differences between procapsid-free and procapsid-bound gp8 subunits are also apparent in Raman markers which monitor environments of tyrosine and tryptophan side chains. Temperature-resolved Raman spectroscopy of the empty procapsid shell reveals three distinct structural transitions for the gp5 subunits. The first, which occurs between 50 and 65 °C, is attributed to shell expansion and results in an increase in β-strand secondary structure. The two higher temperature transitions, occurring within intervals of 70−80 and 80−95 °C, respectively, are attributed to partial unfolding of the shell subunit and subsequent shell disassembly. The same gp5 structure transitions are detected for procapsids which contain scaffolding protein. On the basis of the observed thermodynamic coupling between gp8 unfolding and its release from the procapsid, we propose a model for P22 procapsid assembly. Implications of the model for *in vivo* assembly of dsDNA viruses are discussed.

Icosahedral viruses are composed of an outer shell of coat protein and an inner core containing the viral genome. In addition to the obvious role of protecting the encapsidated nucleic acid against environmental insult, such as nuclease digestion or dehydration, the capsid frequently plays a more active role in the viral life cycle. In some cases, the capsid functions as an active component in nucleic acid packaging; in others it mediates adsorption to the host cell. The capsid must be sufficiently robust to withstand environmental stress, yet capable of releasing the packaged nucleic acid by either ejection or dissociation upon receipt of an appropriate signal. The mechanisms by which these diverse functions are expressed in a virion assembly are of interest not only to virologists, but also to structural biologists concerned with self-assembly of supramolecular structures.

The morphogenetic pathways of icosahedral capsids fall into two classes: (i) those in which the coat protein and the nucleic acid copolymerize, typified by SV40 (Liddington et al., 1991) and the T=3 RNA plant viruses (Casjens, 1985), and (ii) those in which a protein shell is formed first and into which the DNA is packaged subsequently, typified by herpes virus (Newcomb et al., 1993 and references therein) and the dsDNA containing bacteriophages (Casjens & Hendrix, 1988; Murialdo & Becker, 1978; Prevelige & King, 1993).

In the case of the bacteriophages, the precursor structure into which the DNA is packaged is termed a procapsid. The interior volume of the procapsid is occupied by multiple copies of the virally encoded scaffolding protein (King & Casjens, 1974; Casjens & Hendrix, 1988). The presence of the scaffolding protein is required to direct the polymerization of the coat protein into a properly dimensioned shell (King et al., 1973; Roy & Murialdo, 1975). Interior cores of scaffolding protein have also been reported for *herpesviridae* (Sherman & Bachenheimer, 1988; Lee et al., 1988) and *adenoviridae* (D'Halluin et al. 1978). The transformation from procapsid to capsid in these virions involves not only the replacement of the scaffolding protein by nucleic acid, but also a substantial conformational change in the coat protein subunits which constitute the outer shell (Prasad et al., 1993; Dokland & Murialdo, 1993). This conformational change yields a more robust particle and results in a 10% increase in the diameter of the capsid, which renders the internal volume sufficient to package the viral genome. The transformation from procapsid to capsid is tightly controlled and triggered by the presence of the viral DNA (Earnshaw & Casjens, 1980).

A well studied procapsid-to-capsid transformation is that of the bacteriophage P22, where genetic, biochemical, and structural data are available. The procapsid comprises 420 molecules of a 47-kDa coat protein (product of viral gene 5

† Part LI in the series Structural Studies of Viruses by Raman Spectroscopy. Supported by NIH Grants GM50776 (G.J.T.) and GM47980 (P.E.P.).

* Author to whom correspondence may be addressed.
‡ University of Missouri−Kansas City.
§ University of Alabama at Birmingham.

⊗ Abstract published in *Advance ACS Abstracts,* March 15, 1996.

0006-2960/96/0435-4619$12.00/0

or gp5)[1] surrounding an inner core of approximately 300 molecules of the 33-kDa scaffolding protein (gp8) (King & Casjens, 1974; Prasad et al., 1993). One of the 12 vertices is differentiated by the presence of a dodecamer of the 90-kDa portal protein (gp1). The gp1 dodecamer forms a conduit through which the viral genome is translocated during both packaging and infection (Bazinet & King, 1985). As the dsDNA is packaged into the procapsid, the scaffolding protein subunits exit intact and recycle to participate in further rounds of assembly (King & Casjens, 1974).

The transformation from procapsid to capsid has been studied by biochemical, calorimetric, spectroscopic, and electron microscopic (EM) methods. Gentle heating of the procapsid results in a reversible loss of the scaffolding protein, while more extended heating expands the coat protein lattice to the dimensions of the mature virion capsid (Galisteo & King, 1993). Cryo-EM in combination with image analysis reveals holes in the procapsid structure at 28 Å resolution (Prasad et al., 1993). These holes, located at the centers of all hexameric coat protein clusters, may form the channels through which the scaffolding protein exits during DNA packaging. As the DNA is packaged, the diameter of the viral capsid increases from 500 to about 560 Å and the holes are closed. Raman spectroscopy of the procapsid and capsid has demonstrated that this transformation is most likely achieved by a hinge bending motion within the protein subunit (Prevelige et al., 1993). Although it is clear that this structural transformation occurs during DNA packaging, the mechanism of coupling with DNA entry and scaffolding protein release has not been resolved.

The scaffolding release is critical to DNA packaging. Inhibition of scaffolding release is likely to block viral maturation and is hence an antiviral target. Therefore, it is of interest to define the release step at the molecular level. Although the structural changes that occur upon expansion and their energetics are well described, little is known about the conformational changes required in the coat protein subunits for release of the scaffolding protein. Raman spectroscopy provides an ideal probe of the mechanism of such transformations. It is devoid of scattering artifacts which prevent the applicability of other spectroscopic techniques to particles of this size. The Raman spectrum also provides information about both the protein secondary structure and the environments of key side chains. We have undertaken a detailed study of the structural basis of the temperature induced transformations of P22 particles using Raman spectroscopy. In this paper we characterize the structure and thermostability of isolated scaffolding protein, as well as the corresponding states which are assumed within the procapsid shell. On the basis of the present results, we propose an assembly mechanism which involves coupling between release of the scaffolding protein from the procapsid and unfolding of its secondary structure. The data also identify interactions which may be important in retention of scaffolding subunits within the viral procapsid.

MATERIALS AND METHODS

(1) Preparation of Procapsids, Empty Shells, and Scaffolding Protein. Procapsids, empty shells, and scaffolding protein were prepared as described previously (Prevelige et al., 1988). *Salmonella typhimurium* strain DB7136 was grown to $\approx 4 \times 10^8$ cells/mL in superbroth and infected with P22 strain 2^-*amH200*/13^-*am H101* at moi = 5 and grown at 37 °C for 4 h. The cells were chilled on ice, harvested by low speed centrifugation, and frozen in 50 mM Tris/20 mM $MgCl_2$. The cells were lysed by three freeze/thaw cycles in the presence of saturating quantities of chloroform and 1 mM PMSF (phenylmethanesulfonyl flouride). DNase was added to a final concentration of 100 μg/mL, and digestion was continued for 30 min at 37 °C. Cell debris was removed by centrifugation, and the pellet was resuspended in an equal volume of 100 mM EDTA, pH 7.6, frozen, and thawed. The resuspended pellet was centrifuged at 11 000 rpm for 15 min in a Ti-45 rotor, the supernatants were combined, RNase was added to a final concentration of 10 μg/mL, and digestion was continued for 30 min at 37 °C. Debris was pelleted by centrifugation at 11 000 rpm in a Ti-45 rotor for 20 min at 4 °C.

The procapsids were harvested by centrifugation at 35 000 rpm in a Ti-45 rotor for 45 min at 4 °C. The harvested procapsids were resuspended in 14 mL of 50 mM Tris/25 mM NaCl/2 mM EDTA, pH 7.6, and applied to a Sephacryl S-1000 column (volume $\approx$ 200 mL) equilibrated and developed with the same buffer. The procapsid containing fractions were initially located visually by turbidity and confirmed by SDS−PAGE. The procapsid containing fractions were pooled and the procapsids harvested by centrifugation and resuspended in 50 mM Tris/25 mM NaCl, pH 7.6. The procapsids were further purified by banding on a CsCl step gradient using CsCl solutions with densities of 1.4, 1.3, and 1.2 g/cm^3. The procapsids banded at 1.3 g/cm^3 and were harvested by dilution and centrifugation.

The empty shells were prepared from procapsids which had not undergone the CsCl step by repeated extraction with 0.5 M GuHCl at 4 °C, followed by centrifugation. The scaffolding protein was collected from this 0.5 M GuHCl and purified as described previously (Prevelige et al., 1988).

(2) Raman Spectroscopy. The procapsid solution (2.5 mg/mL) was centrifuged at 95 000 rpm for 15 min in a Beckman Airfuge using rotor A-95. The resulting pellet was rinsed and resuspended in 20 μL of 50 mM sodium phosphate/25 mM NaCl buffer, pH 7.5, to achieve a final concentration of about 70 mg/mL. A 10 μL aliquot was sealed in a Kimax #34504 glass capillary. Similarly, the scaffolding protein solution was concentrated to 50 mg/mL for Raman spectroscopy. Samples were thermostated at the temperatures specified (Thomas & Barylski, 1970). Raman spectra were collected on a Spex Model 1877 triple spectrograph (Spex Industries, Metuchen, NJ) equipped with a liquid nitrogen cooled CCD detector (Model ST130, Princeton Instruments, Princeton, NJ). Typically, 30−60 exposures of 1 min each were averaged to produce the spectra shown below.

Procedures for computation of Raman difference spectra of P22 constituents have been described (Prevelige et al., 1990, 1993). Additionally, to compare the observed spectrum of the procapsid with the synthesized spectral sum of its constituents, Raman intensities were normalized with respect to the 621 cm^{-1} band of phenylalanine. The synthesized spectrum was constructed by taking into account both the amino acid compositions of the coat (gp5) and scaffolding (gp8) subunits and their average stochiometric ratio (420:100) in the procapsid, as estimated by quantitative SDS−PAGE. We also employed a linear least-squares

[1] Abbreviations: CD, circular dichroism; DSC, differential scanning calorimetry; EM, electron microscopy; gp5, bacteriophage P22 gene 5 product (major coat protein); gp8, bacteriophage P22 gene 8 product (scaffolding protein); GuHCl, guanidine hydrochloride.

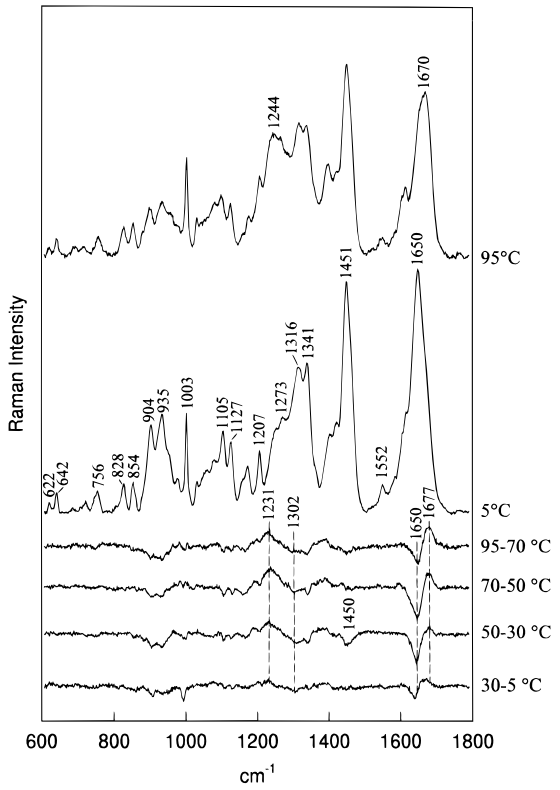

FIGURE 1: Raman spectra of the P22 scaffolding protein (gp8) at 5 °C (second trace from top) and 95 °C (top trace), and difference spectra corresponding to the temperature intervals 95−70, 70−50, 50−30, and 30−5 °C. Intensities are normalized to the spectrum at 5 °C. Experimental conditions are described in the text.

protocol (Pelikan et al., 1994) to minimize the spectral differences between procapsid and constituents. This procedure, which is free of potential normalization errors, was compensated for buffer contributions and baseline artifacts by including the latter in the fitting protocol. Both the intensity-normalization and least-squares procedures yielded identical results.

(3) Circular Dichroism. Scaffolding protein was prepared for CD spectroscopy at 55 μM in 50 mM sodium phosphate, 25 mM NaCl, pH 7.5. The solution was placed in a 0.1 mm cylindrical quartz cuvette and thermostated at the indicated temperatures. CD spectra were collected in the region 185−245 nm on a Jasco J-720 spectropolarimeter (Japanese Optical Corporation, Tokyo, Japan) with 2 nm bandpass, 1 nm wavelength step, 2 s response time and 10 nm/min scanning speed. The instrument was calibrated with a standard solution of *d*-camphor sulfonic acid (Yang et al., 1986). Quantitative analysis of CD spectra was performed by a standard least squares protocol using a set of calibration spectra in the wavelength interval 200−240 nm as described (Yang et al., 1986).

RESULTS AND INTERPRETATION

(1) Structural Properties of the P22 Scaffolding Protein. Raman spectra of aqueous solutions of the scaffolding protein (gp8) were collected over the temperature interval 5−95 °C at increments of 5 and 10 °C. Representative data are shown in Figure 1. At 5 °C, the Raman spectrum of gp8 is dominated by an intense amide I band centered near 1650 cm^{-1}, which is diagnostic of a predominantly α-helical secondary structure (Chen & Lord, 1974). The conformationally informative amide III region of the spectrum (1230−1340 cm^{-1}) also exhibits bands in the interval 1275−1300 cm^{-1}, as expected for an α-helical protein. Additionally, a distinct feature centered at 935 cm^{-1}, assigned to skeletal C−C and C−N vibrations, indicates that the prevailing peptide bond geometry is within the conformation characteristic of α-helix. These results confirm earlier preliminary findings (Thomas et al., 1982). Other prominent bands in the gp8 Raman spectrum are assignable to specific amino acid side chains, as indicated in Table 1.

Table 1: Raman Band Assignments for P22 Coat (gp5) and Scaffolding (gp8) Proteins

gp5		gp8		
frequency (cm^{-1})	relative intensity	frequency (cm^{-1})	relative intensity	assignment[a]
621	0.83	622	0.51	*F6b*
643	0.74	642	0.90	*Y6b*
700	0.55	687	0.30	AmV, σ(C−S)
756	2.32	756	0.98	*W18*
826	1.03	828	1.22	*Y1 + Y16a*
851	1.31	854	1.25	*Y1 + Y16a*
877	1.15	879	0.7	*W17*
902	1.78	904	3.65	sc
937	2.27	935	4.08	σ(C−C$_\alpha$), bk
954	2.22			σ(C−C), sc
975	2.10	978	1.48	sc
1003	10.0	1003	4.13	*F12*
1012	3.30	1011	1.00	*W16*
1032	3.36	1032	1.37	*F18a*
		1060	1.79	σ(C−O), δ(CH$_3$)
1081	2.38	1081	2.25	δ(C−O), δ(CH$_3$)
1102	2.45	1105	3.38	sc
1126	3.05	1127	2.94	W13, sc σ(C−C)
1157	1.58			δ(CH$_3$)
1174	1.76	1174	1.99	*Y9a*, δ(CH$_3$)
1207	3.55	1207	2.56	*F7a, Y7a*
1242	5.42	1257	3.48	AmIII strand
1270	4.40	1273	3.92	*Y7a′*, AmIII helix
1319	5.19	1316	5.99	AmIII helix, sc
1341	5.85	1341	6.15	*W25 + W33/W28 + W29*
1361	2.73	1362	2.06	*W25 + W33/W28 + W29*
1401	3.51	1406	3.21	σ(CO$_2^-$)
		1423	3.77	δ(CH$_2$)
1450	9.33	1451	9.47	δ(CH$_2$)
1551	2.67	1552	1.19	W3
1584	1.44	1587	1.54	*F8b, W2*
1605	3.36	1606	3.31	F8a
1616	3.21	1617	4.19	*Y8a, W1*
		1650	10.00	AmI helix
1663	9.93			AmI strand

[a] Entries in italics indicate normal modes of tryptophan (W), tyrosine (Y), or phenylalanine (F), numbered according to Austin et al. (1993) and references therein. Other abbreviations: Am, amide; sc, nonaromatic side chain; σ, bond stretching vibration of a specific group (in parentheses); δ, deformation vibration of a specific group (in parentheses); bk, unspecified vibration of the polypeptide backbone.

Circular dichroism (CD) spectra, collected at 10 °C, also demonstrate that the dominant secondary structural motif is α-helix (Figure 2). Quantitative analysis of the CD spectrum by a least-squares method (Yang et al., 1986) gives the following estimates: 37 ± 3% α-helix, 30 ± 6% random coil, 33 ± 6% β-turns, and virtually no β-strand. These results are in accord with those obtained previously by Teschke et al. (1993).

The data of Figure 1 show that although gp8 is highly α-helical at physiological temperatures, the secondary structure is thermolabile. The structure of gp8 is observed to change gradually over the temperature range 10−95 °C. (The transition remains reversible below 70 °C.) The change in secondary structure is from an α-helix to a disordered chain. Similar results are obtained by CD spectroscopy, as shown

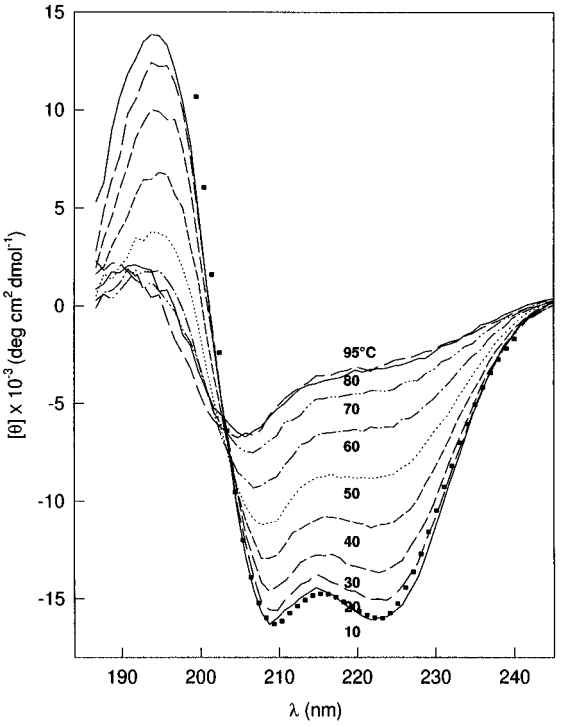

FIGURE 2: CD spectra (185−245 nm) of the P22 scaffolding protein as a function of temperature between 10 and 95 °C. Solid symbols (■) represent the CD profile corresponding to a least-squares fit of the experimental curve to 37 ± 3% α-helix, 33 ± 6% β-turns, and 30 ± 6% random coil (Yang et al., 1986).

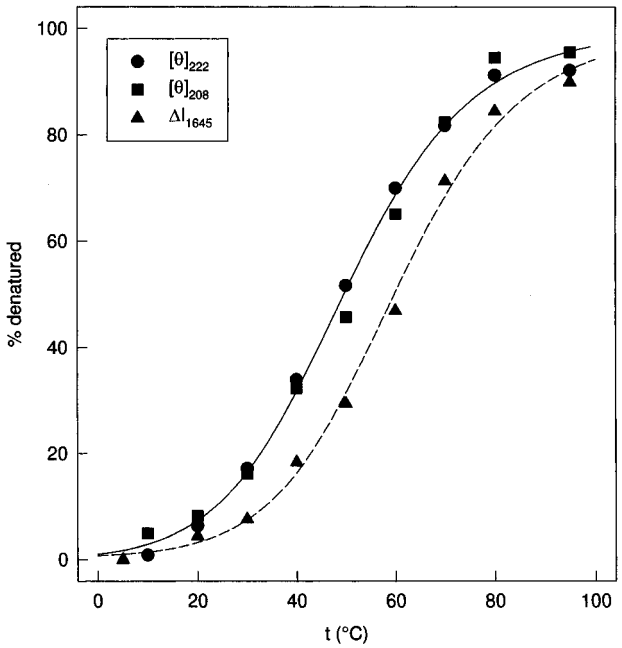

FIGURE 3: Secondary structure melting profiles of the P22 scaffolding protein as monitored by spectral markers of α-helicity. Changes of CD ellipticities at 222 and 208 nm and of Raman amide I intensity at 1650 cm^{-1} were used to calculate the degree of denaturation [$y_d = 100 \times (I_t - I_n)/(I_d - I_n)$, where I_d and I_n are spectral intensities corresponding to fully denatured and native states, respectively]. The CD (solid line) and Raman (broken line) curves correspond to a two-state equilibrium model (Cantor & Schimmel, 1980).

in Figure 2. The relatively noncooperative melting behavior of the protein is reflected in the temperature profiles of the Raman amide I α-helical secondary structure marker (1650 cm^{-1}) and CD ellipticities at 222 and 208 nm (Figure 3). In the course of this secondary structure transition, we observe little or no change in the intensities of Raman marker bands assigned to specific side chains. These results indicate that, despite the definitive transformation of secondary structure, the side chain environments of subunit domains are little affected. Because more significant changes in side chain environments are expected if the subunits aggregate or undergo tertiary structure change, we conclude that neither aggregation nor substantial loss of tertiary structure takes place over the temperature range investigated. The observed denaturation of gp8 secondary structure without alteration of tertiary structure suggests that the scaffolding subunit is not a typical globular protein.

Table 2: Thermodynamic Parameters for Thermal Unfolding of P22 Scaffolding Protein

method	ΔH_u (kJ·mol^{-1})	ΔS_u (J·mol^{-1}·K^{-1})	T_m (°C)
CD	67 ± 5	200 ± 20	49.6 ± 1.6
Raman	72 ± 7	217 ± 22	60 ± 2

We have analyzed the temperature profiles obtained from CD and Raman spectroscopy using a two-state equilibrium unfolding model to obtain an apparent enthalpy change with unfolding (ΔH_u). The data are shown in Figure 3. No statistically significant temperature dependence of either ΔH_u or ΔS_u is observed, in accordance with the apparent lack of unfolding cooperativity. The number of unfolding cooperativity units is $\Delta H_{vH}/\Delta H_u \approx 1$. The thermodynamic parameters determined for the unfolding transition are listed in Table 2. Although we observe a nominal increase in the thermostability of gp8 secondary structure with increasing protein concentration (compare T_m values obtained by CD and Raman spectra, Table 2), there is no apparent increase in the unfolding cooperativity.

(2) Structural Properties of the Coat Protein Subunit in P22 Empty Shells. The P22 empty shells are derived from the procapsid by selective extraction of the scaffolding protein using 0.5 M GuHCl. The shells remain topologically closed, and the overall subunit disposition is identical to that of procapsids which contain the scaffolding protein (Prasad et al., 1993; B. D. Greene and P. Thuman-Commike, personal communication). Previous studies utilizing Raman spectroscopy have shown that the P22 coat protein subunit (gp5) is rich in β-strand (Thomas et al., 1982; Prevelige et al., 1990, 1993), and the data obtained in this study confirm earlier results. Figure 4 displays Raman spectra of aqueous solutions of P22 empty shells collected over the temperature interval 30−95 °C at increments of 5 and 10 °C. Melting profiles for selected Raman bands are shown in Figure 5. Raman bands of structural significance are listed in Table 1 with corresponding residue assignments.

The temperature dependence of the coat protein Raman spectrum (Figures 4 and 5) is consistent with two structural transitions identified previously by DSC (Galisteo & King, 1993): The first, which occurs irreversibly between 50 and 65 °C, is shown here to involve a small gain in β-strand structure at the expense of α-helix. Quantitatively, we observe ≈1.9 ± 0.4% intensity decrease for the amide I Raman band at 1650 cm^{-1}, diagnostic of α-helix, and a concomitant ≈1.5 ± 0.4% increase in the amide I Raman band at 1670 cm^{-1}, diagnostic of β-strand conformations. This transition can be attributed to the procapsid shell expansion studied previously (Galisteo & King, 1993). Empty shells heated under similar conditions also show electrophoretic mobility characteristic of the expanded shells (data obtained on 1.8% agarose gels, not shown).

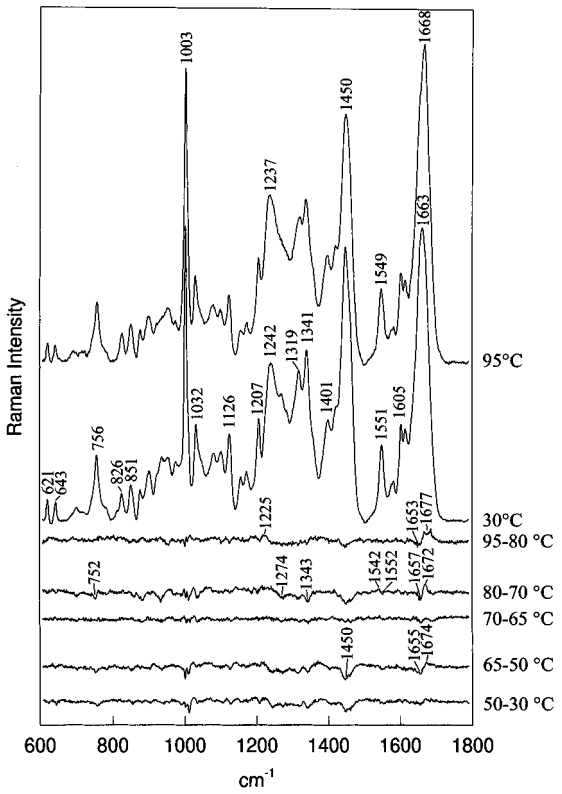

FIGURE 4: Raman spectra of the P22 coat protein (gp5 of the empty procapsid shell) at 30 °C (second trace from top) and 95 °C (top trace), and difference spectra corresponding to the temperature intervals 95−80, 80−70, 70−65, 65−50, and 50−30 °C. Intensities are normalized to the spectrum at 30 °C. Experimental conditions are described in the text.

Figure 4 gives evidence of additional α-helix → β-strand conversion of the coat protein between 70 and 95 °C, as reflected in the 1650 → 1670 cm^{-1} shift in Raman amide I intensity, the 1230 → 1275 cm^{-1} shift in amide III intensity, and the decrease in intensity of the 935 cm^{-1} band. This structure transition apparently includes partial subunit unfolding between 70 and 80 °C and capsid disruption which occurs mainly above 80 °C (Galisteo & King, 1993). Subunit unfolding over the range 70−80 °C is accompanied by a large reorientation of tryptophan side chains, apparent in both Figure 4 and the right panel of Figure 5. Thus, Raman intensity is transferred from 1554 to 1545 cm^{-1} for the prominent tryptophan ring marker (*W3* mode) which is diagnostic of the side chain torsion $|\chi^{2,1}|$ (Figure 4) (Miura et al., 1989). The frequency shift in *W3* indicates a depopulation of conformers with high values of $|\chi^{2,1}|$. Additional changes are observed in tryptophan markers at 753 and 883 cm^{-1}, consistent with altered indole ring environments. Many other spectral differences, particularly within the 1050−1200 cm^{-1} and 1400−1500 cm^{-1} regions, accompany capsid disruption. These indicate extensive rearrangements of aliphatic side chains.

The thermal denaturation of the shell subunit is completed with the final loss of subunit α-helicity between 80−95 °C and corresponding increases in β-strand and irregular or random chain structures. Denaturation is also accompanied by many changes in Raman bands assigned to nonaromatic side chains. On the other hand, no appreciable changes are observed in tryptophan marker bands above 80 °C. From the amide I and amide III profiles it can be concluded that this high temperature transformation does not result in complete loss of subunit secondary structure. It is likely that, at the high protein concentrations employed here, the denatured subunits aggregate, resulting in the observed increase of β-strand secondary structure.

All three phases of the transition distinguished by Raman spectroscopy are irreversible and can be correlated with transitions characterized previously by DSC (Galisteo & King, 1993).

(3) Structural Properties and Thermostability of the P22 Procapsid. Raman spectra of aqueous solutions of P22 procapsids were collected over the temperature interval 30−95 °C at increments of 5 and 10 °C. Representative data are shown in Figure 6. Intensity changes in the amide I region (1650−1670 cm^{-1}) and for the tryptophan *W3* mode (1540−1550 cm^{-1}) are compared with those for the empty procapsid shell in Figure 5. The broad denaturation profile of the procapsid reflects the overlap of the denaturation

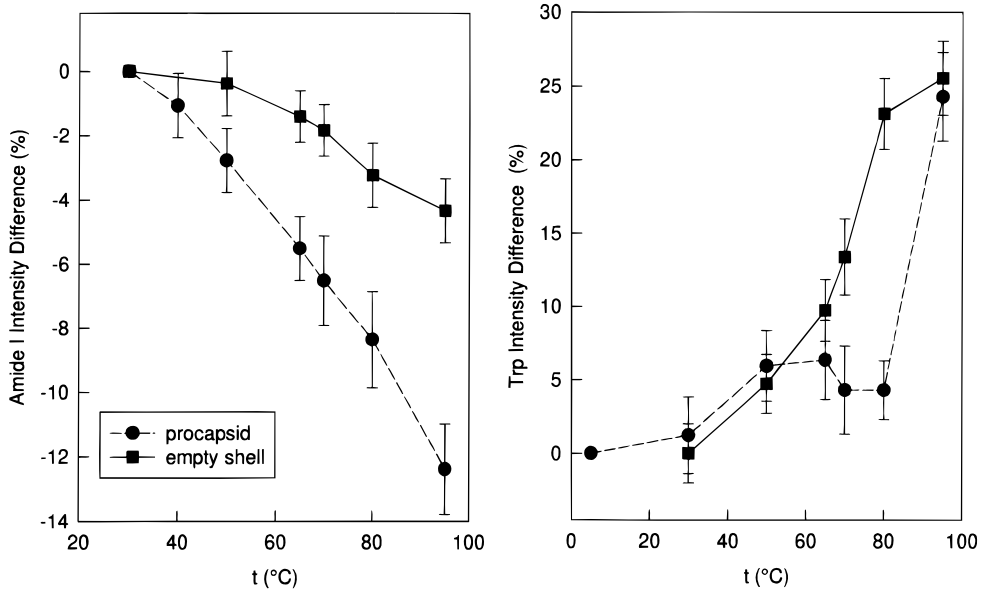

FIGURE 5: Melting profiles of the procapsid shell (gp8/gp5) and empty shell (gp5) as monitored by the percentage decrease in intensity of the Raman amide I α-helix marker at 1650 cm^{-1} (left panel) and by the intensity change of the tryptophan marker near 1540−1555 cm^{-1} (right panel). Intensity changes in the amide I and tryptophan bands were determined from data of Figures 4 and 6. Error bars were determined from average deviations in two or more independent experiments.

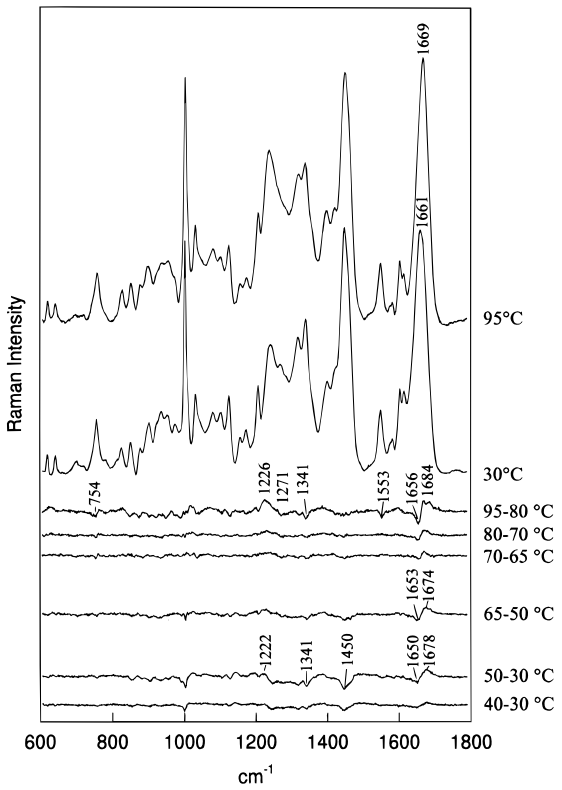

FIGURE 6: Raman spectra of the P22 procapsid (gp8/gp5) at 30 °C (second trace from top) and 95 °C (top trace), and difference spectra corresponding to the temperature intervals 95−80, 80−70, 70−65, 65−50, 50−30, and 40−30 °C. Intensities are normalized to the spectrum at 30 °C. Experimental conditions are described in the text.

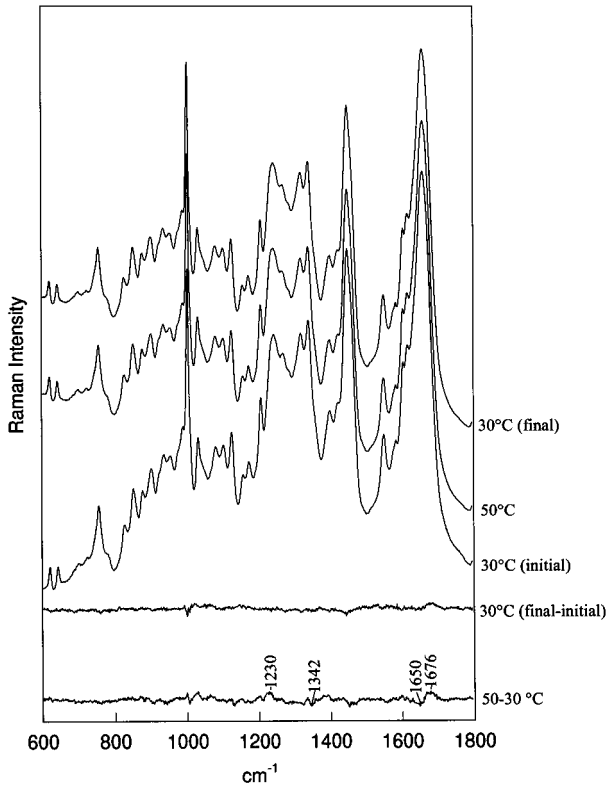

FIGURE 7: Demonstration of reversibility in the transition of the procapsid between 30 and 50 °C. From top to bottom: final spectrum of procapsid at 30 °C, after heating to 50 °C and slow cooling; spectrum at 50 °C; initial spectrum at 30 °C; computed difference between final and initial spectra at 30 °C; computed difference between spectra at 50 and 30 °C.

profile of scaffolding protein with that of the empty procapsid shell. The temperature profile of the *W3* mode of tryptophan reveals an additional procapsid transition between 30 and 50 °C not seen for either the scaffolding protein alone or the empty shells. This transition represents indole ring reorientations for a small population of tryptophans (≈5% of Trp residues) from $|\chi^{2,1}| \approx 110°$ to $|\chi^{2,1}| \approx 80°$. It is accompanied by a decrease in α-helicity and increase in β-strand conformation. Such a secondary structure change is not observed for the empty procapsid shell (Figure 5, left). Other spectral changes of the procapsid (difference bands at 1127 and 1450 cm^{-1}, Figure 6) are due to aliphatic side chain reorientations and are also observed for the empty procapsid, indicating they are likely due to the coat protein. In contrast to the free scaffolding protein alone, in which the conformational changes take place gradually with increasing temperature (Figures 1 and 3), 80% of the conformational changes accompanying the 30−50 °C transition take place between 40 and 50 °C (Figures 5 and 6). This transition is completely reversible, as demonstrated by the virtual identity of procapsid spectra collected before and after heating (Figure 7).

For the empty shell (gp5), we have noted that a net change in tryptophan side chain orientations ($|\chi^{2,1}|$) occurs between 70 and 80 °C (Figures 4 and 5). Surprisingly, the comparable transition takes place in the procapsid at somewhat higher temperature (80−95 °C). This may reflect a subtle difference between the organization of gp5 subunits in shells prepared by GuHCl treatment and those generated by thermal release of the scaffolding protein. It is also possible that the released and denatured gp8 subunits interact in some manner with the shells at 80−95 °C.

If there are no changes in the structures of the coat protein lattice and scaffolding protein subunits upon exit, it should be possible to reconstruct the spectrum of the procapsid at any given temperature by summing spectra of the empty shells (gp5) and scaffolding protein (gp8) at the same temperature, each weighted according to its mass composition in the procapsid and normalized according to its known amino acid composition, as described in the Materials and Methods section. An illustration for data collected at 30 °C is given in Figure 8, which shows that it is not possible to exactly represent the procapsid spectrum as a sum of constituent spectra. The same is true at other temperatures between 30 and 60 °C. This constitutes evidence that coat subunits of the empty shell and scaffolding subunits, when segregated from one another, are structurally different than when combined in the assembled procapsid. Such evidence implies interaction between coat and scaffolding subunits of the native procapsid. Further discussion of this result is given in the following section.

(4) Interaction of Coat and Scaffolding Subunits in the Procapsid. In Figure 8 we compare the observed procapsid spectra with the spectra synthesized as indicated in the preceding section. The resulting difference spectra provide an interesting insight into coat and scaffolding protein interactions. At 30 °C most of the observed difference bands can be assigned to specific side chains (Table 1). For example, the intensity differences at 758, 1204, and 1543 cm^{-1} are due to tryptophan and indicate perturbation of the Trp side chain upon interaction of gp8 and gp5 within the procapsid. The intensity redistribution of the tyrosine Fermi doublet, at 850 and 830 cm^{-1} (Siamwiza et al., 1975), also implicates the phenolic groups in the gp8/gp5 interaction.

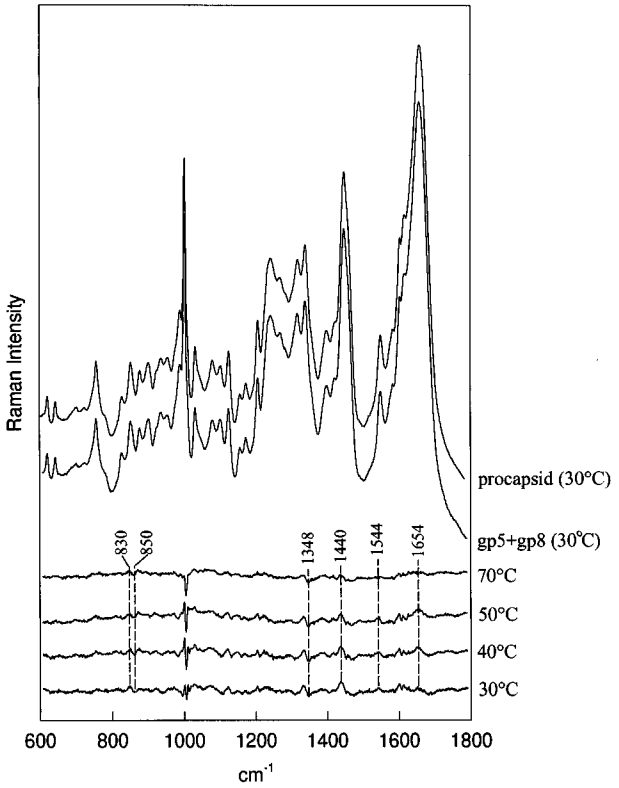

FIGURE 8: Comparison of the Raman spectrum of the P22 procapsid (gp8/gp5, top) with the sum of spectra of the P22 scaffolding protein and empty procapsid shell (gp8 + gp5, second from top), all at 30 °C. The spectrum of the sum was generated by least-squares matching to the spectrum of the complex, so as to minimize differences in spectral intensities and frequencies. Possible contributions of the baseline and buffer of each spectrum were taken into account in the least-squares optimization (Pelikan et al., 1994). Also shown are difference spectra between the procapsid and its constituents at 70, 50, 40, and 30 °C, as labelled.

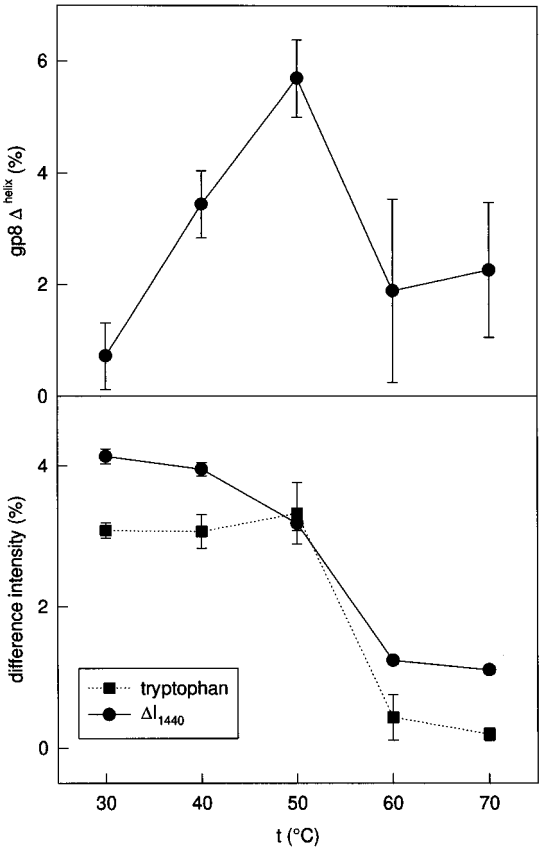

FIGURE 9: Top panel: Temperature dependence of the *excess* α-helicity of scaffolding protein in the P22 procapsid. The excess is defined as the additional α-helical secondary structure of the gp8 subunit in the procapsid vis-à-vis the extracted state, each monitored by the Raman amide I intensity at 1650 cm^{-1} (from Figure 8). A similar result is obtained for the amide III α-helix marker at 1348 cm^{-1} (not plotted). Bottom panel: Temperature dependence of intensity differences between selected Raman markers of the procapsid and its sum of constituents (from Figure 8). Data points are shown for the tryptophan marker near 1544 cm^{-1} (dotted line) and for the aliphatic side chain marker near 1440 cm^{-1} (solid line). A similar result is obtained for the tyrosine doublet near 850 and 830 cm^{-1} (not plotted).

The data suggest that tyrosines in the procapsid complex serve as stronger hydrogen bond acceptors than tyrosines of the separated proteins (Siamwiza et al., 1975). The difference peaks observed at 1601 and 1614 cm^{-1} support this interpretation (Rogers et al., 1992; Austin et al., 1993). The difference peaks observed at 1332 and 1438 cm^{-1} are assigned to methylene deformation modes of aliphatic side chains (Lin-Vien et al., 1991). These intensity changes may reflect altered side chain packing or solvent interactions (Thomas et at., 1983). Similarly, differences in the 1050−1200 cm^{-1} region are likely due aliphatic side chain reorientations (Lin-Vien et al., 1991).

All of the above noted differences occur below 50 °C. Melting profiles for those of tryptophan (1543 cm^{-1}) and aliphatic side chains (1440 cm^{-1}) are shown in the lower panel of Figure 9. The profiles display a rather abrupt transition near 50 °C, which is consistent with the expected highly cooperative exit of scaffolding protein from the procapsid (Galisteo & King 1993). Quantitatively, however, the differences account for only a small fraction of the parent band intensities, indicating that only a limited number of side chains participate in the interactions.

The differences observed in the 1630−1700 cm^{-1} region upon heating from 30 to 50 °C are assigned to the amide I mode and represent altered secondary structure of gp5 and/or gp8 upon procapsid assembly. On the basis of the positive peak located at 1652 cm^{-1}, we conclude that the average secondary structure of the procapsid assembly is more α-helical than its constituents. The trough observed at 1682 cm^{-1} indicates replacement of the helical stucture by β-strand upon disassembly. Based upon the α-helix to β-strand transition observed for free gp8 (see above) and the high α-helicity of gp8, these changes occur most probably in gp8. Interestingly, the differences increase in magnitude with increasing temperature between 30 and 50 °C, achieve a maximum at 50 °C, and then sharply attenuate with further increase of temperature between 50 and 60 °C. This is illustrated in the upper panel of Figure 9 by the temperature dependence of the excess α-helicity, as measured by the 1652 cm^{-1} difference intensity (normalized with respect to the total amount of gp8 α-helical secondary structure).

The Figure 9 profile demonstrates that the secondary structure of gp8 is fully retained within the procapsid up to 50 °C. Thus, both the secondary and tertiary structural transitions appear to be more cooperative for the procapsid assembly than for its isolated constituents. The apparent cooperativity of main chain unfolding is evidently linked to gp8 exit, shown previously to be a cooperative phenomenon (Galisteo & King, 1993). The cooperativity in altered side chain environments, on the other hand, can be attributed to specific interactions between gp5 and gp8.

DISCUSSION AND CONCLUSIONS

(1) The Empty Procapsid Shell. The change in conformation of the gp5 main chain accompanying heat-induced expansion of the empty procapsid shell is small. Simple analysis of the amide I difference implies a 1.9 ± 0.4% decrease in α-helix and a concomitant 1.5 ± 0.4% increase in *β*-strand. This is qualitatively and quantitatively similar to the conformational difference measured in gp5 when Raman signatures of empty procapsid shells and empty mature shells are compared with one another (Prevelige et al., 1993). Thus, the subunit conformational change accompanying the heat-induced expansion of procapsid shells appears to mimic very closely the subunit conformational change which accompanies the expansion triggered by DNA packaging. Although the well-defined vertices of the native empty shell (Prasad et al., 1993) are not evident in the heat-expanded shell (Galisteo & King, 1993), the respective subunit conformations are virtually identical in the two types of expanded particles.

In addition to the above conformational change, we have observed two additional structural transformations in the empty shell. One occurs between 70 and 80 °C and involves loss of main chain α-helicity, as well as alteration of the average conformation and environment of tryptophan side chains. We believe this structural transformation corresponds to the partial denaturation of gp5 observed by DSC at 70−80 °C (Galisteo & King, 1993). The final structural transformation coincides with shell disassembly and gp5 denaturation above 90 °C. It is characterized by a dramatic increase in *β*-strand secondary structure as well as large scale changes in side chain environments typical of protein denaturation (Thomas et al., 1983).

(2) The Procapsid. We have observed a procapsid transition at 40−50 °C involving loss of α-helicity as well as changes in selected side chain environments. Because a similar transition does not occur in the empty shell, we assign the structure changes to the scaffolding subunits upon their release from the procapsid (Galisteo & King, 1993). This transition is completely reversible, as expected for the exit and reentry of scaffolding protein (Greene & King, 1994).

The 70 °C Raman spectrum of the procapsid is virtuallly identical to a linear combination of spectra of isolated gp8 and expanded empty shells (Figure 8), but cannot be satisfactorily approximated by any linear combination involving the spectrum of the nonexpanded empty shell (data not shown). Thus, we conclude that the thermally induced procapsid shell expansion is complete at 70 °C.

Further, above 70 °C the scaffolding and coat protein subunits do not appear to interact, as judged by the additivity of their constituent spectra in the procapsid. The only exception is a reorientation of tryptophan residues, observed between 70 and 80 °C for the empty shell and at higher temperatures for the procapsid. This may reflect the different histories of samples prepared by heat treatment and GuHCl extraction, rather than a substantive gp5/gp8 interaction.

(3) The Scaffolding Protein. Following thermal denaturation, the α-helical secondary structure of gp8 is converted to *β*-strand. Using a simple two-state approximation, the enthalpy of unfolding (ΔH_u) has been estimated from Raman and CD melting data as 67 ± 5 and 72 ± 7 kJ/mol, respectively. Within this approximation, we find no dependence of ΔH_u or ΔS_u on temperature, which suggests that $\Delta C_p \approx 0$. The small value of ΔH_u and the absence of a change in heat capacity agree with calorimetric experiments (Galisteo & King, 1993).

The broad, noncooperative melting profile of gp8 resembles the denaturation of a polypeptide lacking the hydrophobic core typical of globular proteins (Privalov, 1979). The absence of a typical hydrophobic core is also demonstrated by the accessibility of all peptide NH groups of gp8 to rapid deuterium exchange (data not shown). These findings suggest a highly flexible tertiary structure comprising multiple α-helical domains. Sedimentation analysis shows further that gp8 is a prolate ellipsoid with an axial ratio of 9:1 (Fuller & King, 1981). We propose that gp8 consists of segmented α-helices connected by flexible domains and lacks a hydrophobic core. The gp8 sequence is extraordinarily rich in proline and acidic and basic residues, which is consistent with the proposed structural model.

Even at the high gp8 concentration employed for Raman spectroscopy (50 mg/mL versus 1.7 mg/mL for CD), we observe no large increase in cooperativity and no apparent temperature dependence of ΔH_u and ΔS_u. On the other hand, the melting temperature of 50 °C from CD data is increased to 60 °C in the Raman experiments, suggesting some effect of concentration. This may reflect less favorable interactions between gp8 molecules in the thermally unfolded state at high concentration, which is consistent with the high charge density of the gp8 subunit.

In contrast to gp8 denaturation, the release of scaffolding subunits from the procapsid is highly cooperative and is accompanied by an excess heat capacity (Galisteo & King, 1993). This implies the formation of hydrophobic interactions involving gp8 within the procapsid. The Raman spectra indicate that many side chains, including tryptophans and tyrosines, undergo interactions specific to procapsid assembly. The magnitude of the spectral perturbations is small, however, thus implicating only a limited number of side chains. Although we cannot distinguish whether the perturbed residues reside on gp5 or gp8 or both, such interactions presumably lead to sequestration of subunit domains from solvent and convey cooperativity to scaffolding protein release.

Raman spectroscopy also indicates that only *the native* α-helical form of gp8 is bound to the procapsid structure. Below the exit temperature, procapsid interactions stabilize the native conformation. Upon exit, the conformation of gp8 is governed by the equilibrium between its native and denatured states.

(4) Procapsid Assembly Model. A simple model for procapsid assembly is illustrated in Figure 10. Salient features of this model, proposed on the basis of previous and present results, are the following: (1) Assembly is initiated by recognition between the highly α-helical scaffolding (gp8) subunits and the highly *β*-stranded coat (gp5) subunits. (2) gp8 subunits interact specifically with gp5 subunits, forming the correct architecture of the procapsid. Interaction of gp8 and gp5 in the procapsid results in thermostabilization of the α-helical conformation of gp8 (Figure 8). (3) The procapsid-bound scaffolding protein is in equilibrium with similarly folded but unbound and more thermolabile gp8 subunits (Figures 1−3). (4) The unbound gp8 subunits represent in turn an equilibrium between unfolded and incompletely folded forms. The ensemble of folded and unfolded gp8 subunits is available for subsequent rounds of gp5 recognition and procapsid assembly.

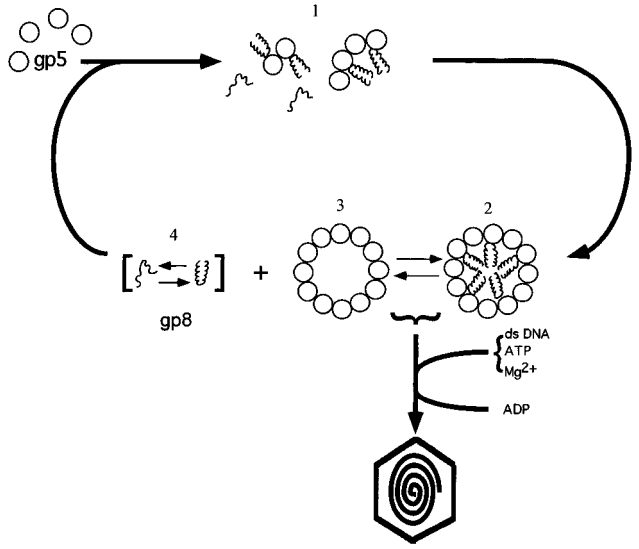

FIGURE 10: A model for assembly of the P22 procapsid. Salient features include: (1) Initiation of assembly by molecular recognition between gp8 and gp5; (2) thermostabilization of gp8 secondary structure through formation of procapsids of the correct architecture, which are in equilibrium with (3) empty shells and (4) an equilibrium mixture of folded and incompletely folded gp8 subunits. The latter are available for subsequent rounds of assembly. The *in vitro* transition from (2) to (4) is accomplished *in vivo* by the packaging of dsDNA, shown by the path at the lower right. *In vivo* packaging does not generate the empty shell (3), but a closely related mature shell incorporating gp5 subunits of the same apparent secondary and tertiary structures (Prevelige et al., 1993).

The procapsid assembly model of Figure 10 is consistent with a number of observations based upon physicochemical and genetic experiments. First, the exit of a scaffolding subunit from the procapsid shell is coupled to its folding equilibrium. Thus, the *in vitro* denaturation of gp8 by chemical (GuHCl, urea) or physical (pressure and temperature) means is effective in driving its release from the procapsid. The *in vivo* counterpart of this driving force is presumably the dsDNA packaging event. The packaged genome competes for the same excluded volume and binding sites otherwise occupied by the scaffolding protein. As expected, the latter phenomenon shifts the system (gp8 subunits) toward the ensemble of folded and unfolded states of gp8 which become available for further rounds of assembly *in vivo*. Finally, because *in vivo* packaging of DNA is coupled with irreversible expansion of the procapsid shell, the exit of scaffolding protein is an essentially irreversible process.

We have characterized the solution conformation of the scaffolding protein of bacteriophage P22, both when bound in the native procapsid and when free from association with any other viral factor. The thermostability of the gp8 structure has been characterized for these two states of assembly. Specific side chains which play a role in stabilizing the native α-helical conformation of procapsid-bound gp8 have been identified. We have proposed a simple, thermodynamically based pathway to account for gp8/gp5 recognition, procapsid assembly, and capsid expansion. A key element of the model is the proposed coupling between gp8 folding/unfolding and shell binding/release equilibria. Future work will focus on identifying structural domains of gp8 in which the distinct functional roles of folding, recognition of gp5, and release from the procapsid are localized.

REFERENCES

Austin, J., Jordan, T., & Spiro, T. G. (1993) in *Advances in Spectroscopy* (Clark, R. J. H., & Hester, R. E., Eds.) Vol. 20, pp 55−127, Wiley, London.

Bazinet, C., & King, J. (1985) *Annu. Rev. Microbiol. 39*, 109−129.

Cantor, C. R., & Schimmel P. R. (1980) *Biophysical Chemistry, Part III: The behavior of biological macromolecules*, pp 1077−1078, W. H. Freeman, San Francisco.

Casjens, S. (1985) in *Virus Structure and Assembly* (Casjens, S., Ed.) pp 88−95, Jones and Bartlett, Boston.

Casjens, S., & Hendrix R. W. (1988) in *The Bacteriophages* (Calendar, R., Ed.) Vol. 1, pp 15−90, Plenum, New York.

Chen, M. C., & Lord, R. C. (1974) *J. Am. Chem. Soc. 96*, 4750−4752.

D'Halluin, J.-C. M., Martin, G. R., Torpier, G., & Boulanger, P. (1978) *J. Virol. 26*, 357−363.

Dokland, T., & Murialdo, H. (1993) *J. Mol. Biol. 233*, 682−694.

Earnshaw, W., & Casjens, S. (1980) *Cell 21*, 319−331.

Fuller, M. T., & King, J. (1981) *Virology 112*, 529−547.

Galisteo, M. L., & King, J. (1993) *Biophys. J. 65*, 227−235.

Greene, B., & King, J. (1994) *Virology 205*, 188−197.

King, J., & Casjens, S. (1974) *Nature 251*, 112−119.

King, J., Lenk, E. V., & Botstein, D. (1973) *J. Mol. Biol. 80*, 697−731.

Lee, J. Y., Irmieve, A., & Gibson, W. (1988) *Virology 167*, 87−96.

Liddington, R. C., Yan, Y., Moulai, J., Sahli, R., Benjamin, T. L., & Harrison, S. C. (1991) *Nature (London) 354*, 278−284.

Lin-Vien, D., Colthup, N. B., Fateley, W. G., & Grasselli, J. G. (1991) *The Handbook of Infrared and Raman Characteristic Frequencies of Organic Molecules*, Academic Press, London.

Miura, T., Takeuchi, H., & Harada, I. (1989) *J. Raman Spectrosc. 20*, 667−671.

Murialdo, H., & Becker, A. (1978) *Microbiol. Rev.*, 529−576.

Newcomb, W. W., Trus, B. L., Booy, F. P., Steven, A. C., Wall, J. S., & Brown, J. C. (1993) *J. Mol. Biol. 232*, 499−511.

Pelikan, P., Ceppan, M., & Liska, M. (1994) *Applications of Numerical Methods in Molecular Spectroscopy*, CRC Press, Boca Raton.

Prasad, B. V. V., Prevelige, P. E., Marietta, E., Chen, R. O., Thomas, D., King, J., & Chiu, W. (1993) *J. Mol. Biol. 231*, 65−74.

Prevelige, P. E., & King, J. (1993) in *Progress in Medical Virology* (Melnick J., Ed.) Vol. 40, pp 206−221, Karger, Basel.

Prevelige, P. E., Thomas, D., & King, J. (1988) *J. Mol. Biol. 202*, 743−757.

Prevelige, P. E., Thomas, D., King, J., Towse, S. A., & Thomas, G. J., Jr. (1990) *Biochemistry 29*, 5626−5633.

Prevelige, P. E., Thomas, D., Aubrey, K. L., Towse, S. A., & Thomas, G. J., Jr. (1993) *Biochemistry 32*, 537−543.

Privalov, P. L. (1979) *Adv. Protein Chem. 33*, 167−241.

Rodgers, K. R., Su, C., Subramaniam, S., & Spiro, T. G. (1992) *J. Am. Chem. Soc. 114*, 3697−3704.

Roy, P., & Murialdo, H. (1975) *Virology 64*, 247−263.

Sherman, G., & Bachenheimer, S. L. (1988) *Virology 163*, 471−480.

Siamwiza, M. N., Lord, R. C., Chen, M. C., Takamatsu, T., Harada, I., Matsuura, H., & Shimanouchi, T. (1975) *Biochemistry 14*, 4870−4876.

Teschke, C. M., King, J., & Prevelige, P. E., Jr. (1993) *Biochemistry 32*, 10658−10665.

Thomas, G. J., & Barylski, J. (1970) *Appl. Spectrosc. 24*, 463−464.

Thomas, G. J., Jr., Li, Y., Fuller, M. T., & King, J. (1982) *Biochemistry 21*, 3866−3878.

Thomas, G. J., Jr., Prescott, B., & Day, L. A. (1983) *J. Mol. Biol. 165*, 321−356.

Yang, J. T., Chuen-Shang, C. W., & Martinez, H. M. (1986) in *Methods in Enzymology*, Vol. 130, pp 208−269, Academic Press, New York.

BI952793L